PAPER

Crack detection sensor layout and bus configuration analysis

IOP Publishing Smart Materials and Structures
Smart Mater. Struct. **23** (2014) 055021 (8pp) doi:10.1088/0964-1726/23/5/055021

Crack detection sensor layout and bus configuration analysis

Nathan Sharp[1], Alan Kuntz[2], Cole Brubaker[3], Stephanie Amos[4], Wei Gao[5], Gautam Gupta[5], Aditya Mohite[5], Chuck Farrar[5] and David Mascareñas[5]

[1] Purdue University, West Lafayette, IN 47905, USA
[2] University of New Mexico, Albuquerque, NM 87131, USA
[3] Colorado State University, Fort Collins, CO 80523, USA
[4] Georgia Tech, Atlanta, GA 30332, USA
[5] Los Alamos National Laboratory, Los Alamos, NM 87545, USA

E-mail: dmascarenas@lanl.gov

Received 30 October 2013, revised 9 January 2014
Accepted for publication 30 January 2014
Published 1 April 2014

Abstract
In crack detection applications large sensor arrays are needed to be able to detect and locate cracks in structures. Emerging graphene-oxide paper sensing skins are a promising technology that will help enable structural sensing skins, but in order to make use of them we must consider how the sensors will be laid out and wired on the skin. This paper analyzes different sensor shapes and layouts to determine the layout which provides the preferred performance. A 'snaked hexagon' layout is proposed as the preferred sensor layout when both crack detection and crack location parameters are considered. In previous work we have developed a crack detection circuit which reduces the number of channels of the system by placing several sensors onto a common bus line. This helps reduce data and power consumption requirements but reduces the robustness of the system by creating the possibility of losing sensing in several sensors in the event that a single wire breaks. In this paper, sensor bus configurations are analyzed to increase the robustness of the bused sensor system. Results show that spacing out sensors in the same bus as much as possible increases the robustness of the system and that at least 3 buses are needed to prevent large segments of a structure from losing sensing in the event of a bus failure. This work is a preliminary effort toward enabling a new class of 'networked materials' that will be vitally important for next generation structural applications. 'Networked materials' have material properties related to information theoretic concepts. An example material property is 'bandwidth' per unit of material that might indicate the amount of information the material can provide about its state-of-health.

Keywords: sensing skin, robust, sensor layout, crack detection, bus

(Some figures may appear in colour only in the online journal)

1. Introduction

In many structural health monitoring (SHM) applications, the monitoring system is looking for cracks in the structure which is indicative of damage. In some cases exciting and/or monitoring with vibro-acoustic or thermal signals can be an effective method for monitoring cracks. In many situations, however, especially where the system is remote and weight, size, and power consumption are limited (e.g. unmanned aerial systems, UAS), these traditional SHM strategies are not as effective.

A number of crack monitoring systems are currently being explored by researchers. Distributed fiber optic systems have been developed to detect cracks as well as measure temperature and strain in multiple locations [1–5]. The distributed sensors are suitable for large structural applications, which is important in crack detection. However, these systems have not found widespread usage due to insufficient resolutions,

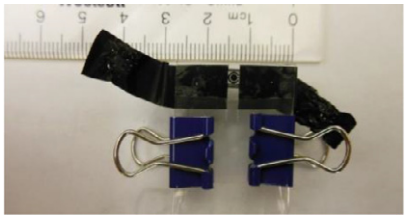

Figure 1. Graphene-oxide capacitor.

weak detectable signals, and cumbersome demodulation systems [6]. Another strategy is to use tomography to estimate the conductivity which can detect cracks since a crack will cause a loss of conductivity [7, 8]. The advantage of this strategy is that the entire area within the tomography boundary has sensing capability. The disadvantages of this strategy is that estimating conductivity from boundary values is an inverse problem and inverse problems have inherent limitations in size and resolution [9]. Elastomeric capacitive sensing skins have also recently been developed [10] and hold promise for health monitoring of civil infrastructure. A fourth strategy for crack detection is to embed or print wires on a structure and monitor for loss of connection, which would indicate a crack [11]. The advantages of this system are that it is the least expensive option and can easily be scaled to almost any size. One disadvantage of this method is that, unlike fiber optic systems, there is no way to know where a wire has been cut. Another disadvantage is that, unlike the tomography method, the entire area does not have sensing capability (a crack must go through a wire). These disadvantages can be minimized by choosing smart sensor shapes and layouts. However, to the best of our knowledge no one has analyzed how the sensor shape and layout affects its crack detection and crack location performance. Since sensing skin systems would likely be most effective in cases where maintenance and resources are limited, it is important that sensors are created and arranged in such a way as to maximize information and robustness. This paper will analyze effects of sensor shape and layout in the wire-based sensor skins only.

2. Overview of the graphene-oxide sensing skin

The motivation to develop new wiring and sensor layout schemes comes from the recent emergence of graphene-oxide paper materials [12]. One particularly interesting use of graphene-oxide papers is the construction of novel super capacitors [13] by reducing graphene-oxide with a laser. An example of such a super capacitor is shown in figure 1. This super capacitor is patterned on a free-standing sheet of graphene-oxide paper using a laser-reduction patterning technique. However, graphene-oxide can also be deposited as a film on other materials, as well as combined with other materials such as cellulose to create new composite materials. Laser reducing graphene-oxide allows the electrical properties of the resulting reduced graphene-oxide to be tuned. For instance, graphene-oxide is not conductive, but reduced graphene-oxide is conductive depending on the amount of reduction the graphene-oxide is subjected to. Figure 2 shows

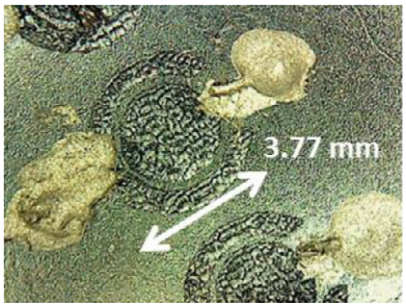

Figure 2. Healthy graphene-oxide capacitor on cellulose paper substrate.

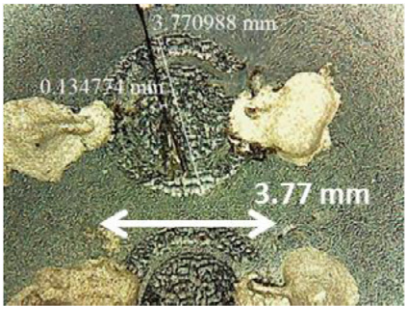

Figure 3. Damaged graphene-oxide capacitor on cellulose paper substrate. Damage is induced in the capacitor by cutting through it with a knife. The knife cut is 0.135 mm wide.

a super capacitor that is laser-patterned on a film of graphene-oxide that is deposited on cellulose paper. There are a number of important emerging structural applications of paper-based structures. A particularly interesting application is the need for intelligent tamper-indicating seals that can be remotely interrogated. Materials based on graphene-oxide present a particularly interesting way to realize this next generation of seal technology. The concept is that reduction by laser patterning can be used to modify the electrical properties of graphene oxide to create an array of capacitors on a sheet of graphene-oxide paper material. The flexibility of laser patterning allows for the creation of individualized capacitor arrays that can be used to uniquely identify each seal. A sensing scheme can then be used to monitor the capacitance of the sensors in the array. When a capacitor is damaged or cut as shown in figure 3 the capacitance of the array is changed and an indication of tampering or damage is made. Since graphene-oxide can be either deposited as a film using spray-coating techniques, or be formed into a free-standing paper or paper composite it is conceivable that a sensing skin made from this material can be incorporated into the layers of a fiber-reinforced polymer composite or a be deposited on a metallic structure. Graphene-oxide shows promise as a structural sensing skin material.

3. Engineering considerations for a graphene-oxide sensing skin

In order to use laser-reduced graphene-oxide super capacitors as a sensing skin material two important considerations must be made. First, what measurement mechanism will be used to

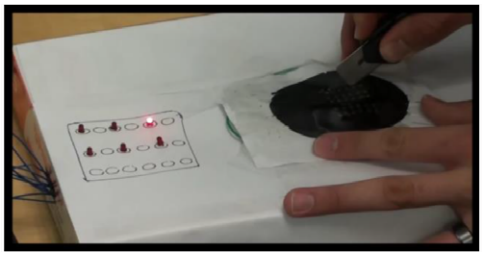

Figure 4. The graphene-oxide–cellulose composite skin being damaged by a through-cut with a knife. The red LED indicates the presence and location of the damage.

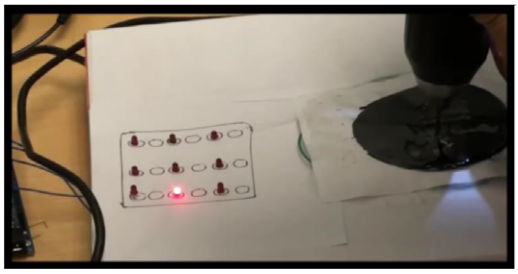

Figure 5. Epoxy-coated graphene-oxide–cellulose skin being damaged by being drilled through. The red LED indicates the damage location.

collect the current capacitance values of the skin, and second, how will the sensors and communication/power lines be laid out and incorporated into the skin.

To address the first question, graphene-oxide can be configured as either a resistive or capacitive sensor using laser-reduction patterning techniques. Capacitors and resistor sensor elements with a variety of different geometries can be patterned onto a graphene-oxide layer. The resistance/capacitance of these sensor elements will change when a crack propagates through the material and cuts the sensors. This change in resistance/capacitance is then used as an indicator of damage. An example of a graphene-oxide–cellulose composite skin being used as a damage indicator in this manner is shown in figures 4 and 5. The graphene-oxide–cellulose skin is damaged by being cut through and drilled through respectively. In figure 5 the graphene-oxide–cellulose skin is coated in epoxy to help illustrate how this material might work in a structure made from fiber-reinforced-plastic.

Addressing the second question concerning how the sensors and communication/power lines will be laid out is the primary focus of the research undertaken in this paper. We decided that important features we would like to have include an overall robustness of the system to damage. If a portion of the sensing skin is damaged the whole system performance should degrade gracefully. A small cut to one portion of the system should not lead to whole sections of the skin structure losing the ability to detect damage. It would be preferable for the negative effects of damage to be localized to only areas where the damage occurs. Working towards developing a sensor layout that achieves these goals is the focus of this research effort.

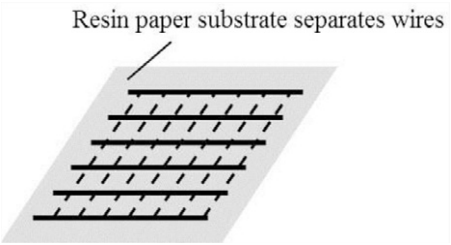

Figure 6. Previously proposed grid layout.

4. Sensor layout analysis

In this section we are primarily concerned with the design and layout of capacitive/resistive sensors that can be used to detect cracks. The sensors considered here consist of a curvilinear profile that experiences a change in either capacitance/resistance when it is cut through. This change in capacitance/resistance is used to indicate the presence of damage in that sensor. The curvilinear nature of these sensors allows for a sensor layout pattern that consists of any combination of curvilinear elements. It is clear that some layout patterns will have superior properties for detecting cracks than others, and finding high-performance crack detection patterns is the primary focus of this section. Zhang *et al* [11] proposed a grid patterned crack detection sensor layout shown in figure 6. In this figure, the solid lines represent conductive paths on the front side of the resin paper substrate and the dashed lines represent conductive paths on the back side. Throughout the paper this convention will be used to represent lines which intersect but do not touch. While this layout was shown to be able to detect and locate cracks, no analysis was done to determine how this sensor layout performs compared to other layouts. In order to do this analysis, fitness metrics must be outlined so that performance can be compared quantitatively. The most obvious performance metric of a crack detection sensor is how well it detects cracks. Therefore, one goal of the sensor layout and shape design is to minimize the crack length at which a crack is detected. Another important job of the sensor (at least in some applications) is locating the crack. Therefore, the other goal of the sensor layout and shape design is to minimize the area of the crack location uncertainty when a crack is detected. A third goal is to minimize the number of sensors needed to achieve the first two goals.

The first step in analyzing sensor performance is to find appropriate bounding cases. One way to get very good crack detection performance with very few sensors is to take the grid pattern and connect all the vertical lines together and all the horizontal lines together, as shown in figure 7. This will be referred to as the ‘snake’ pattern for convenience sake. The detection performance of this pattern is only limited by how closely neighboring lines are spaced together and only uses 2 sensors no matter how large the sensor area. The downside of this pattern is that there is no crack location information. The other bounding case is a layout with the smallest possible location uncertainty with a fixed number of sensors per unit area. To find this, a layout that can has sensors that tile and pack together tightly is needed. Both squares and hexagons (where

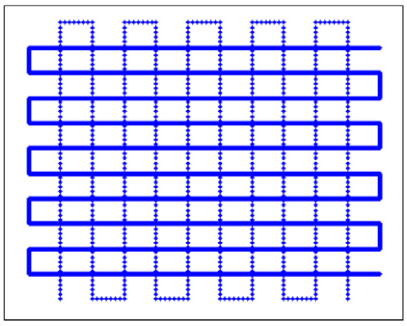

Figure 7. 'Snake' sensor layout.

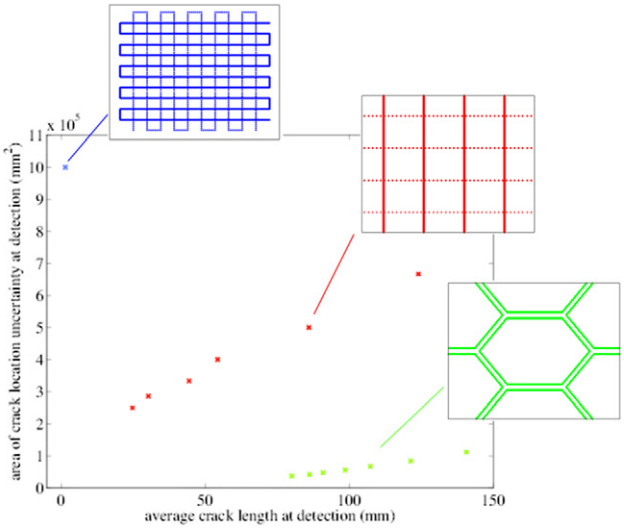

Figure 8. Performance plot of three different sensor layouts.

the sensor would be the boundary of the square/hexagon) pack together perfectly and therefore offer the same location uncertainty performance, but hexagons offer slightly better crack detection performance (see appendix A) so a hexagonal layout was used.

Figure 8 shows the crack detection performance and location performance for the three sensor layouts described above. The horizontal axis shows the average crack length at detection, while the vertical axis shows the area of the location uncertainty of the crack at detection. The area of location uncertainty is defined as the area of the surface where the crack could possibly be located. Figure 9 shows an example of the area of location uncertainty in a grid pattern with a detected crack. An ideal sensor would be at the origin. A surface with an area of 1 m^2 was populated with sensors of the three different layouts shown in figure 8. For this simulation only two dimensions were considered: all cracks were treated as penetrating the surface completely. This assumption would be realistic for very thin structures or structures where only a surface needs to be monitored (perhaps a composite laminate), but would not be accurate in bulk structures where depth also needs to be considered. It would also be valid in the case of a tear in an intelligent tamper-indicating seal. To be conservative the thickness of the cracks has been neglected. A Monte Carlo analysis was performed by simulating 5000 through-thickness

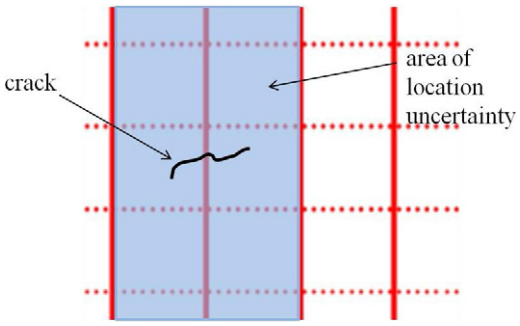

Figure 9. Area of location uncertainty example.

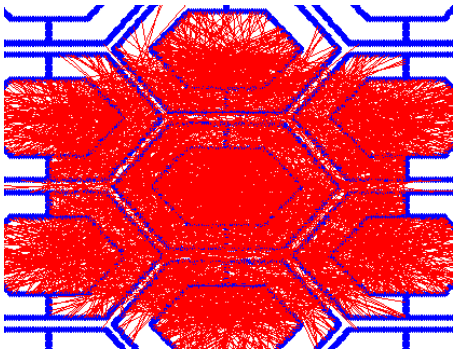

Figure 10. Example of the simulation for determining sensed crack lengths. In this image a sensor consisting of two nested hex profiles is shown to give some sense of how cracks were allowed to propagate.

cracks in random locations and the cracks were propagated linearly in a random direction until the crack touched a sensor. The locations of the cracks were uniformly distributed over a circular area in the center of the simulated plate. The radius of the circle is such that it covers one complete hexagonal sensor, and half of the width of the adjacent sensors. Figure 10 shows a representative example of the simulation area for a hex-style sensor. In this case the sensors consist of two nested hex profiles. The results for this particular sensor configuration are not reported in this paper, but we use this example because it most clearly shows the nature of how the simulation was carried out. The direction of propagation of the cracks was also uniformly distributed from 0° to 360°. The cracks were propagated linearly until they crossed a sensor outline. Upon crossing a sensor outline we decide the sensor has been detected and stop that simulation. The average length before a crack crosses a sensor is displayed along the horizontal axis of figure 8. In order to show how the values are a function of the number of sensors per unit area, the crack simulation was run with 6, 8, 10, 12, 14, 16, and 18 sensors covering the 1 m^2 area (except for the snake layout since it always has 2 sensors by definition). More sensors for the same area implies lower average crack length and lower area uncertainty, so the lower left values represent the highest number of sensors. Therefore, from lower left to upper right respectively, each value can be compared directly. This plot shows that, as expected, the snake pattern performs best at crack detection but worst at locating the crack, the hexagonal pattern performs best at locating the

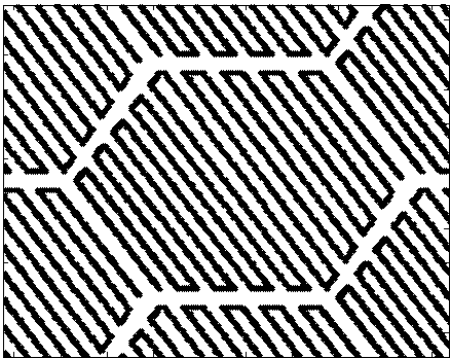

Figure 11. 'Snaked hexagon' layout.

crack but worst at detecting it, and the grid pattern is in between for both.

The advantages of the snake pattern and the hexagonal pattern can be combined to get the advantage of each layout by patterning 'snaked' sensors in a hexagonal shape, as shown in figure 11. Figure 12 shows the performance plot shown in figure 8 but also includes the snaked hex layout included (note that plots showing layout shapes are not to scale relative to each other). This layout has the same area uncertainty as the hexagonal pattern and crack detection performance which is almost as good as the snake pattern. Therefore, this plot shows that the snake layout is the best if crack location information is not important and the snaked patterned shape layout is best if location information is important. Note that, unlike the grid and hexagon layouts, the crack detection performance of the snaked hexagon layout is not very dependent on the number of sensors. Instead it is dependent on the spacing of the snaked lines. The crack detection performance for both the snake pattern and snaked hexagon layouts could be better or worse than that reported in figure 8 depending on what spacing is used. In this simulation, a spacing of 2 mm was used between lines for both sensor layouts. The constraints that would determine the best spacing would be cost (smaller spacing means more conductor/manufacturing time for laser reduction), the thickness of the conductor, and the length of the conductor before the normal resistance gets too high. Also note that the crack detection performance of the grid pattern would eventually converge to that of the snake pattern if enough sensors were used, but the same performance parameters can be gained using fewer sensors with the snaked hexagon layout.

5. Bus configuration analysis

In previous work we have developed a crack detection system which reduces the number of required, unique communication channels by placing several sensors onto a common bus line. The bus would work by multiplexing the sensors, similar to work which has been done previously [14, 15]. In this case the simplest way to bus the sensors together would be the use of time division multiplexing, where only one of the sensors on each bus is being sensed at any given time and the sensor which is being sensed rotates through all of the sensors on the bus. This helps reduce wiring, number of analog-to-digital

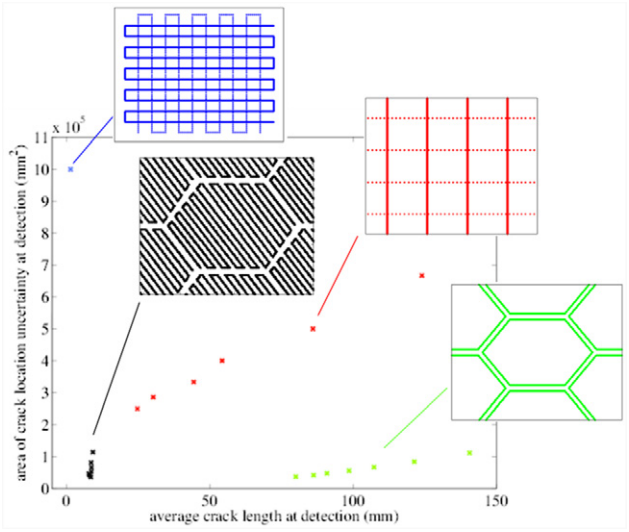

Figure 12. Performance plot with snaked hexagon layout.

converters, bandwidth, and power consumption requirements. Unfortunately this comes at the expense of reducing the robustness of the system by creating the possibility of losing communication with several sensors in the event a bus wire breaks. It is preferable to develop new sensor layouts that degrade gracefully as the individual components of the system fail.

We now consider how to design sensor/bus layouts that are robust against single points of failure. This study is predominantly concerned with the robustness properties of the network one level of abstraction up from the individual sensor performance with respect to layout type considered in the previous section. Based on the results above, a hexagonal pattern was selected to be tested as the sensor type being connected using 2, 3, 4, 6, 8, and 12 unique buses. Since the goal was to prevent allowing a single bus failure to create a region incapable of being observed by the sensors, the sensors were spaced as far apart from each other as possible. For the purposes of the research in this section each hexagon can be thought of as a sensor that is capable of detecting the presence of a crack within it's boundaries. Figure 13 shows the sensor arrangements with 2, 3, and 4 sensors, where hexagons of like colors are connected on the same bus.

The performance of each sensor configuration was tested in the event of a single bus failure. After removing all of the sensors from one of the buses in each case, 10 000 cracks were randomly populated on a sensor skin surface using a uniform distribution on a circle centered in the middle of the simulation area. The cracks were advanced in a random direction (uniformly distributed over 0°–360°) until a crack hit a sensor. In order to simplify the simulation the entire hexagon of each active sensor was considered sensitive to a crack. This simulation was run 10 times for each ordered sensor layout as well as 10 times for a random sensor layout with the same number of broken sensors. The sensor grid was 10 rows and columns, and the simulated cracks were generated a distance away from the edges to prevent edges from skewing the results. Figure 14 shows the sensor layout with 3 buses where one

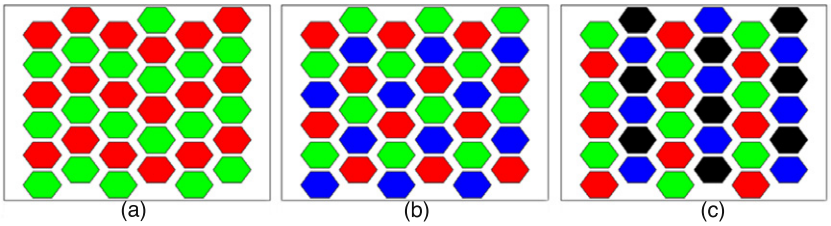

Figure 13. Sensor configurations for (a) 2, (b) 3, and (c) 4 buses.

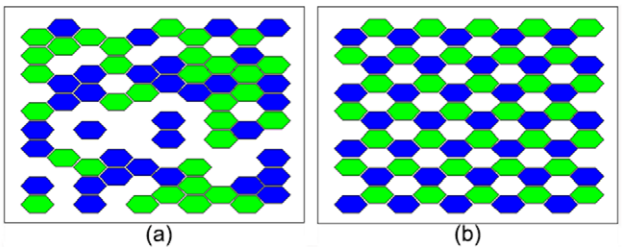

Figure 14. 3-bus sensor configuration for (a) random and (b) ordered cases. In this plot one of the three buses has been rendered inoperable and thus is simply whited out leaving only the two remaining buses.

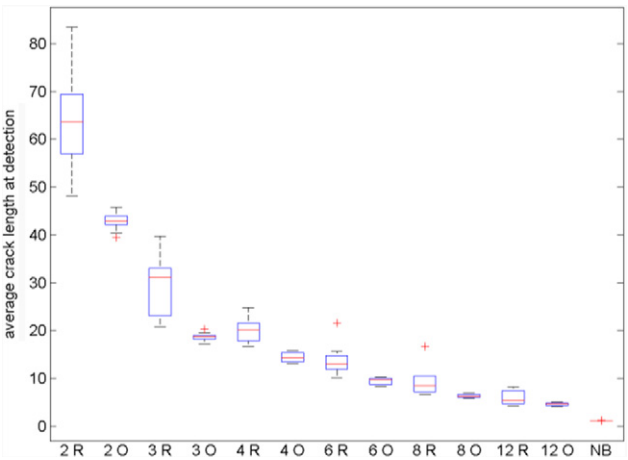

Figure 15. Boxplot results of sensor configuration simulations.

of the buses has been removed for (a) the random case and (b) the ordered case.

Boxplot results for the simulations are shown in figure 15. The labels for each boxplot state the number of buses for the simulated case followed by 'R' for random or 'O' for ordered. The 'NB' label stands for 'not broken', or a fully functional sensing skin. Figure 16 shows the results of each case when all of the crack lengths are averaged to get a single average value. Unsurprisingly, the ordered layouts perform significantly better than the random layouts. The results also show that the skin performance scales roughly linearly with the number of sensors still active except for the 2-bus case. This is because with only 2 buses there is no way to isolate each sensor on a bus from its neighbors so that losing a bus necessarily creates large sensing gaps. These results show that if bus failure is a concern, at least 3 buses should be used. Beyond that there

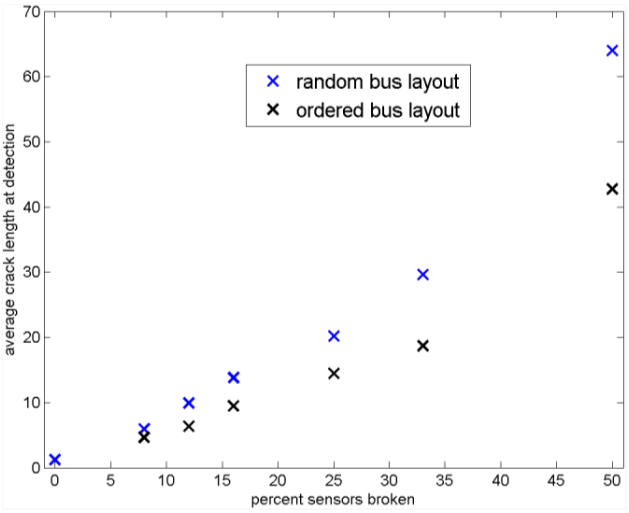

Figure 16. Average crack lengths for several bus configurations.

is a somewhat linear tradeoff between the number of channels in the sensing skin and the skin performance in the case of bus failure. The preferred number of buses depends entirely on the individual application and constraints.

6. Bus wiring layout

In order to realize the proposed robust, sensing skin layouts, it is imperative that a workable method be developed to wire the individual sensors to their respective buses properly. Currently our preferred method of communication from the individual sensors to the centralized processing unit is done using a small number of common communication buses. The concept is that each sensor will have some centralized processing associated with it. This processing capability will also serve to provide communication on the bus. A large number of sensors are connected to each bus and use the same line to communicate with the central processing unit. In order to use common bus line for multi-node communication some scheme must be adopted to regulate communication traffic on the bus. A very common solution is to impose a master–slave relationship between devices on the bus and place the bus lines in an open-drain configuration as is done in I^2C[16]. I^2C is setup using two common bus lines each of which feature a pull-up resistor. Any device on the bus can pull the common bus line low. In this way all nodes on the line can see all the communication traffic that crosses the line. An arbitration scheme is used to make

sure that nodes only send data at appropriate times without causing contention on the bus.

The advantage of using the common bus is that the wiring requirements are significantly reduced. Instead of requiring an individual communication line from each sensor back to the central processing unit, a single communication line can be strung between many sensors located throughout the network. This feature is especially important for developing intelligent materials featuring internal self-sensing capabilities. A properly wired bus layout should have the property that if a small portion of the bus is damaged or cut, the resulting loss of sensor communication is localized to only the damaged portion of the skin. For the case of a single bus connecting all the sensors on the skin, one wiring scheme that features this property is simply a grid with a sensor at each vertex. The conductors used to form the bus can take a variety of forms, but for the purpose of this work we envision printing the conductors on the skin using a conductive ink. For the case of the two buses connecting all the sensors the solution is also fairly straightforward. In this case we take advantage of the fact that the types of sensors we are primarily interested in at this time (graphene-oxide capacitors and resistors) can be patterned on both sides of a sheet of graphene-oxide paper. In order to achieve two buses all we need to do is put one bus and its associated sensors on one side of the graphene-oxide paper, and place the other sensors/bus on the opposite side of the paper. The bus layout on each side of the paper can once again take the form of a simple grid with a sensor located on each vertex. Thus far we have seen though that a 3-bus solution is of interest because it provides both good robustness properties as well as the ability to detect short-length cracks. One wiring layout solution for the 3-bus case featuring sensors with a hexagonal perimeter is shown in figure 17. In this case all the sensors are patterned on both sides of the graphene oxide material. Typically the sensors are patterned into the material using a device such as a Co_2 laser. In this case the laser power can be increased to produce a small hole through the graphene-oxide material at each sensor location. Conductive ink can then printed to fill this hole thus producing a via to electrically connect both sides of the graphene-oxide material. At this point conductive-ink bus traces can be printed onto each side of the graphene-oxide paper. The key to making this work in such a way that sensors across the skin are bused together is to have the bus traces on one side of the paper travel in a direction that is nearly orthogonal to the bus traces on the opposite side of the graphene-oxide paper. By following this procedure and using the bus layout shown in figure 17 it is possible to achieve the use of 3 common buses with this type of sensing skin. Furthermore, each individual bus is designed in such a way that it is actually robust against global failure on its own. Even if an individual sensor on a bus is damaged, or part of the bus itself is damaged, the whole bus will not go down. Only the portion of the bus local to the damage will be affected. Furthermore, exotic manufacturing techniques are not required to realize this design. Another nice feature of this design, is that an electrical connection to the bus can be established from almost anywhere on the edge. There is no need to make specialized arrangements to route bus wires to the connectors for the centralized processor.

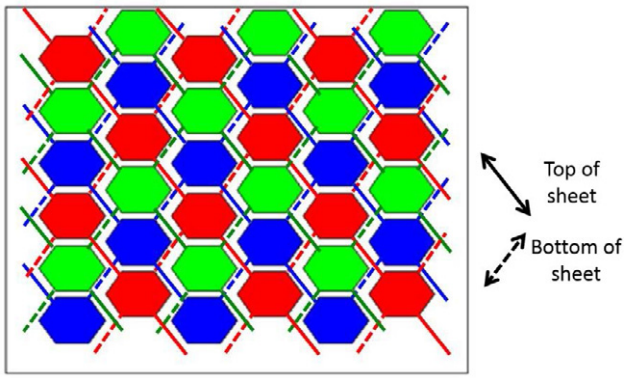

Figure 17. Scheme for wiring the 3-bus sensing skin configuration. Solid lines are bus wires on the top sheet, dashed lines are bus wires on the bottom sheet. Sensors are patterned on each side of the sheet. Bus lines on each side of the sheet run in the same direction.

Work is currently underway to select/develop additional communication protocols to utilize this robust, common bus physical layer. The commonly used I^2C, multimaster, serial, single-ended computer bus [16] would directly be able to use this type of physical layer by simply adding two pull-up resistors for each bus. We are also taking inspiration from the asynchronous address-event representation (AER) for the communication of asynchronous events between a collection of units performing parallel computations [17]. Our goal is to eventually develop a system that can utilize an AER-like protocol to enable asynchronous communication of the presence of damage in a sparse, low-memory, low-power, reactive manner.

7. Conclusions

Crack monitoring skin systems could be a valuable SHM tool in emerging SHM/smart materials applications such as intelligent tamper-indicating seals. In this paper sensor shape was analyzed in order to maximize the crack detection and crack locating abilities for each sensor. In the event that sensors are bussed together to reduce the sensing channel requirements, bus configurations were analyzed to identify ways to make the network robust in the event of a bus failure. Results show that at least 3 buses are desirable to prevent losing sensing capabilities in large segments of a structure. This work is a preliminary effort toward enabling a new class of materials that will be vitally important for future structural health monitoring applications we are referring to as ‘networked materials’. These are materials for which there are materials properties related to information theoretic concepts. An example material property is ‘bandwidth’ per unit of material that might indicate the amount of information the material can provide about its state-of-health. This work will help provide engineering guidance for designing these materials.

Acknowledgments

The authors would like to acknowledge the support of the Los Alamos National Laboratory—Laboratory Directed Research

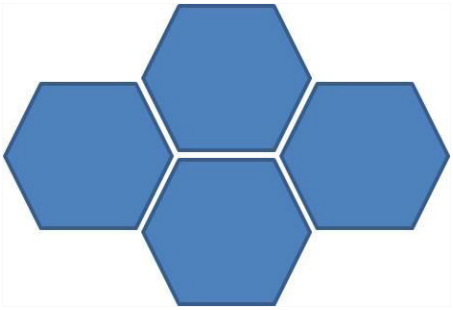

Figure A.1. Hexagonal sensor array.

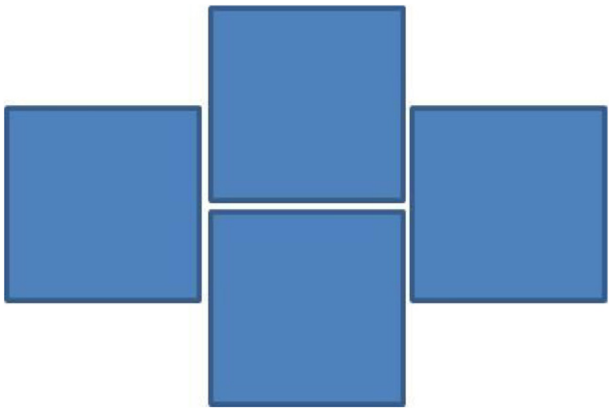

Figure A.2. Square sensor array.

and Development program. Grant no. 20130527ER. We would also like to acknowledge Karen Miller of Los Alamos National Laboratories for encouraging us to explore the use of smart materials for novel, tamper-indicating seal technology.

Appendix

Assume two arrays with equal sensor density, one with hexagonal sensors and one with square sensors. A subset of a hexagonal array is shown in figure A.1 with the horizontal space between the top and bottom sensors showing the longest undetected crack length. Figure A.2 shows the same thing with square sensors. Also assume ideal sensors such that any crack within the sensor in any location will be detected. In this case the only place where cracks can develop undetected is along the boundary of the sensors. Assuming that the spacing between the sensors is small then the longest possible undetected crack in the hexagonal array is approximately one side length, as is the longest possible undetected crack in the square array. Since the area for a hexagon is approximately equal to 2.6 times length squared and the area for a square is equal to the length squared, then the longest undetected crack in the hexagonal array is approximately 1/2.6, or 0.39, times the longest undetected crack in the square array.

References

[1] Inaudi D and Glisic B 2005 Development of distributed strain and temperature sensing cables *Proc. 17th Int. Conf. on Optical Fiber Sensors (Bruges, May 2005)* part 1, pp 222–5
[2] Glisic B and Verma N 2011 *Proc. 8th Int. Workshop on Struct. Health Monitoring* vol 2, pp 1409–16
[3] Yao Y, Tung S-T E, Verma N and Glisic B 2013 *Proc. 9th Int. Workshop on Struct. Health Monitoring* vol 2, pp 2787–94
[4] Hoult N, Bennett P, Stoianov I, Fidler P, Maksimović C, Middleton C, Graham N and Soga K 2009 *Proc. ICE—Civil Eng.* **162** 136–44
[5] Gu X, Chen Z and Ansari F 1999 *J. Intell. Mater. Syst. Struct.* **10** 266–73
[6] Lia H, Lia D and Songa G 2004 *Eng. Struct.* **26** 1647–57
[7] Loh K, Hou T, Lynch J and Kotov N 2009 *J. Nondestruct. Eval.* **28** 9–25
[8] Dharap P, Li Z, Nagarajaiah S and Barrera E 2004 *Nanotechnology* **15** 379
[9] Okamoto Y, Teramachi Y and Musha T 1983 *IEEE Trans. Biomed. Eng.* **30** 749–54
[10] Laflamme S, Kollosche M, Connor J and Kofod G 2013 *J. Eng. Mech.* **139** 879–85
[11] Zhang B, Zhou Z, Zhang K, Yan G and Xu Z 2006 *J. Intell. Mater. Syst. Struct.* **17** 907–17
[12] Dikin D A *et al* 2007 *Nature* **448** 457–60
[13] Gao W, Singh N, Song L, Liu Z, Mohana Reddy A L, Ci L, Vajtai R, Zhang Q, Wei B and Ajayan P M 2011 *Nature Nanotechnology* **6** 496–500
[14] Lopez-Amo M, Blair L and Urquhart P 1993 *Opt. Lett.* **18** 1159–61
[15] Zheng S and Li Y 1997 *Opt. Eng.* **36** 3392–400
[16] NXP Semiconductors 2012 *UM10204 I2C-Bus Specification and User Manual* version 5
[17] 2002 *Extended Address Event Representation Draft Standard* version 0.4